Electronic supplementary information

Formation of porous CC@Fe_xO/Co_3O_4-Cu_xO/CS photocathodes for high power-density zinc-air batteries with reduced charging potentials

Yuhao Zhong, [a] Qian Rong,*[ab] Weibin Zhang, [ab] Xiaobo Feng [ab] and Ting Zhu *[ab]

[a] School of Physics and Electronic Information, Yunnan Normal University, 768 Juxian Street, Kunming 650500, Yunnan, China.

[b] Yunnan Key Laboratory of Optoelectronic Information Technology, Yunnan Normal University, 768 Juxian Street, Kunming 650500, Yunnan, China.

Experimental section

Preparation of CC@Co_3O_4/CS nanosheets

The carbon cloth (CC, 4 × 3 cm²) was pretreated in a mixed solution of HNO_3/H_2SO_4 (volume ratio 1:3) for 24 h. The CC was repeatedly rinsed 5 times with deionized (DI) water and anhydrous ethanol, and then dried in a vacuum oven at 60°C for 12 h to obtain the pretreated CC. A 0.02 mol/mL aqueous solution of 2-methylimidazole and 0.003 mol/mL aqueous solution of $Co(NO_3)_2 \cdot 6H_2O$ were prepared, the two solutions were vigorously stirred and mixed at room temperature. The CC was then immersed in the aforementioned mixture solution and allowed to stand for 12 h. Afterward, the CC was retrieved, thoroughly rinsed with deionized water, and dried overnight at 60°C to obtain the CC@Co-MOF nanosheet array. The nanosheet array was heated to 800°C at a rate of 1 °C·min^{-1} under an Ar/H_2 (19:1), and held at a constant temperature for 2 h. Subsequently, it was further annealed in a muffle furnace at 250°C with a heating rate of 2 °C·min^{-1} for 2 h, yielding the CC@Co_3O_4/CS nanosheets.

Preparation of CC@Fe_xO/Co_3O_4/CS nanosheet arrays

The CC@Co-MOF was immersed in $K_3[Fe(CN)_6]$ aqueous solution (0.05 M) and

allowed to stand for 30 min. The resulting sample was repeatedly rinsed with deionized water and ethanol, then dried overnight in an oven at 60°C to obtain the CC@Co/Fe-MOF nanosheet arrays. Subsequently, it was annealed at 800 °C for 2 h under an Ar/H_2 (19:1) atmosphere with a heating rate of 1 °C·min^{-1}, yielding CC@CoFe-800. The material was further calcined at 250°C in air for 2 h (with a heating rate of 2 °C·min^{-1}) to produce CC@Fe_xO/Co_3O_4/CS nanosheet arrays.

Preparation of CC@Fe_xO/Co_3O_4-Cu_xO/CS composites

A mixture of 240 mg $CuSO_4·5H_2O$ and 147 mg $Na_3C_6H_5O_7·2H_2O$ were dissolved in 80 mL of deionized water under magnetic stirring at 60°C for 15 min. Subsequently, 20 mL of an aqueous NaOH solution (1.25 M) was added dropwise, followed by the slow addition of 50 mL $C_6H_8O_6$ aqueous solution (0.03 M), and stir continuously for 8 min to obtain Cu_xO solution. The CC@CoFe-800 was placed in the as-prepared Cu_xO solution for 1 h. After retrieval, the sample was rinsed with ethanol and deionized water, dried and annealed at 250°C in air for 2 h to obtain the CC@Fe_xO/Co_3O_4-Cu_xO/CS composite.

OER and ORR measurement

All electrochemical measurements were conducted using an V38144 electrochemical workstation (Ivium, the Netherlands) in a standard three-electrode system. The working electrode was the as-prepared sample (dimensions: 1×1.5 cm²), with a platinum foil as the counter electrode and a saturated calomel electrode (SCE) as the reference electrode. The oxygen evolution reaction (OER) tests were performed in 0.1 mol·L^{-1} KOH electrolyte, while the oxygen reduction reaction (ORR) measurements employed 1.0 mol·L^{-1} KOH electrolyte. All reported potentials were converted to the reversible hydrogen electrode (RHE) scale using the Nernst equation.

$$E_{RHE} = E_{SCE} + 0.241 + 0.0591PH$$

The photoelectrochemical measurements were performed using a xenon lamp as the light source, with all tests conducted in a thermostatically controlled water circulation system maintained at 25°C to eliminate photothermal effects.

Fabrication and Testing of ZABs

The CC@Fe_xO/Co_3O_4-Cu_xO/CS was cut into 1.5×1.5 cm^2 pieces to serve as the cathode substrate. A 2×2 cm^2 waterproof membrane and a washed nickel mesh (2.5 × 6 cm^2) were sequentially stacked on its surface, followed by compression to form the composite cathode. The anode consisted of 0.5 mm thick zinc foil (2.5 × 6 cm^2), which was processed by stamping to form a round hole with a diameter of 16 mm for light

exposure. The battery assembly was sealed and secured using three plates and silicone gaskets to ensure structural stability. The electrolyte was an alkaline mixed solution of 6 mol·L^{-1} KOH and 0.2 mol·L^{-1} $Zn(Ac)_2$, which was injected into the battery device through a circulating pump to ensure uniform flow. The photoelectric test was conducted using a 300 W xenon lamp source to simulate solar irradiation. All experiments were carried out under constant illumination conditions to evaluate the photoelectrocatalytic performance of electrode materials.

Materials characterization

The crystal structure of the samples was characterized by X-ray diffraction (XRD, Rigaku D/max 2550, Cu Kα radiation, λ= 0.154 nm). The chemical states and elemental composition were analyzed using X-ray photoelectron spectroscopy (XPS, Thermo Fisher-VG Scientific ESCALAB 250Xi). The microscopic morphology was observed via scanning electron microscopy (SEM, Quanta FEG 250), while the microscopic structure was further resolved by high-angle annular dark-field scanning transmission electron microscopy (HAADF-STEM, Titan G2 60-300). For optical properties, the ultraviolet-visible (UV-Vis) absorption spectra were recorded on a PerkinElmer Lambda 950 spectrophotometer using $BaSO_4$ as a reflectance standard. Photoluminescence (PL) spectra were collected at room temperature using a fluorescence spectrophotometer (QuantaMaster 40, PTI, Canada). In addition, the electron paramagnetic resonance (EPR) test was conducted using a ruker A300 spectrometer at a microwave frequency of 9.85 GHz to study the oxygen vacancies in the samples.

Supplementary figures

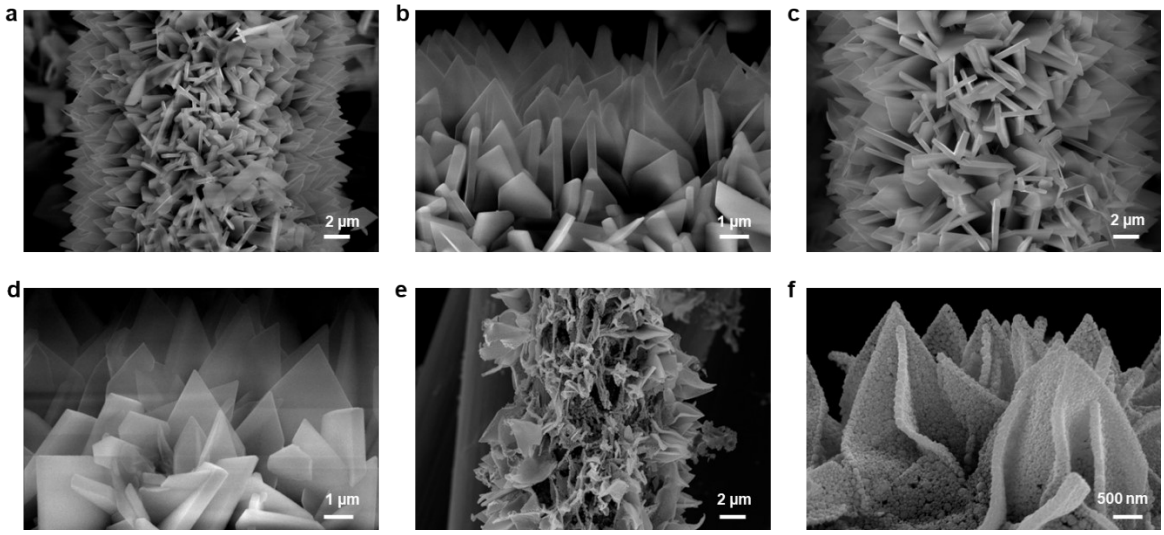

Fig. S1. FESEM images of the CC@Co-MOF (a and b), CC@Co/Fe-MOF (c and d) and CC@CoFe-800 (e and f) samples.

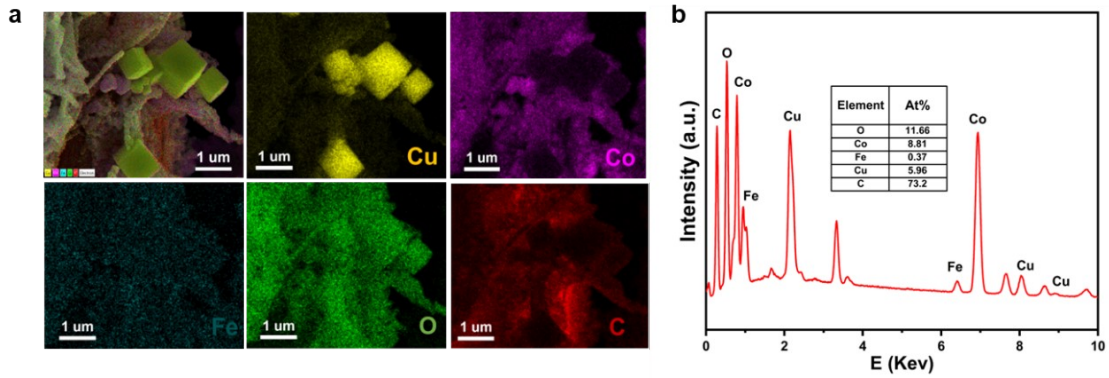

Fig. S2. FESEM element distribution images (a) and EDS spectrum (b) of the CC@Fe_xO/Co_3O_4-Cu_xO/CS.

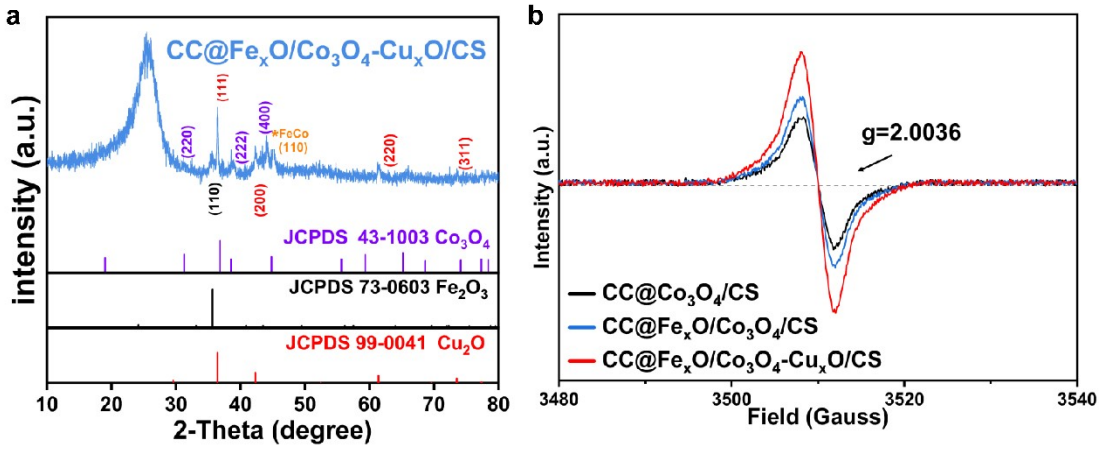

Fig. S3. The XRD pattern (a) and EPR spectra (b) of CC@Fe_xO/Co_3O_4-Cu_xO/CS.

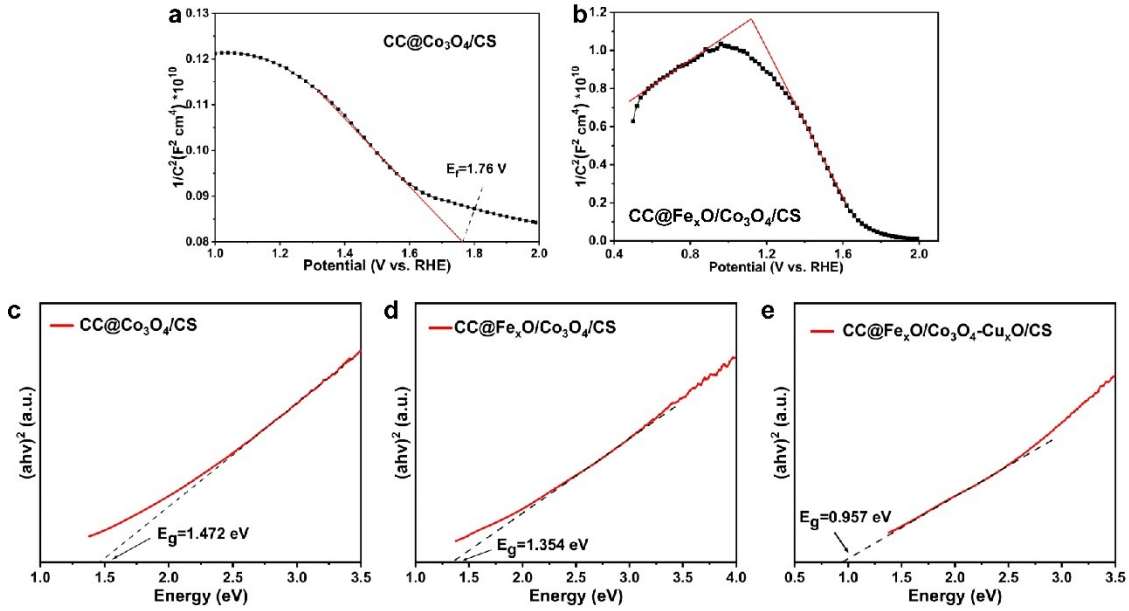

Fig. S4. Mott-Schottky curves (a and b) and bandgap energies (c-e) of CC@Co_3O_4/CS, CC@Fe_xO/Co_3O_4/CS and CC@Fe_xO/Co_3O_4-Cu_xO/CS samples, respectively.

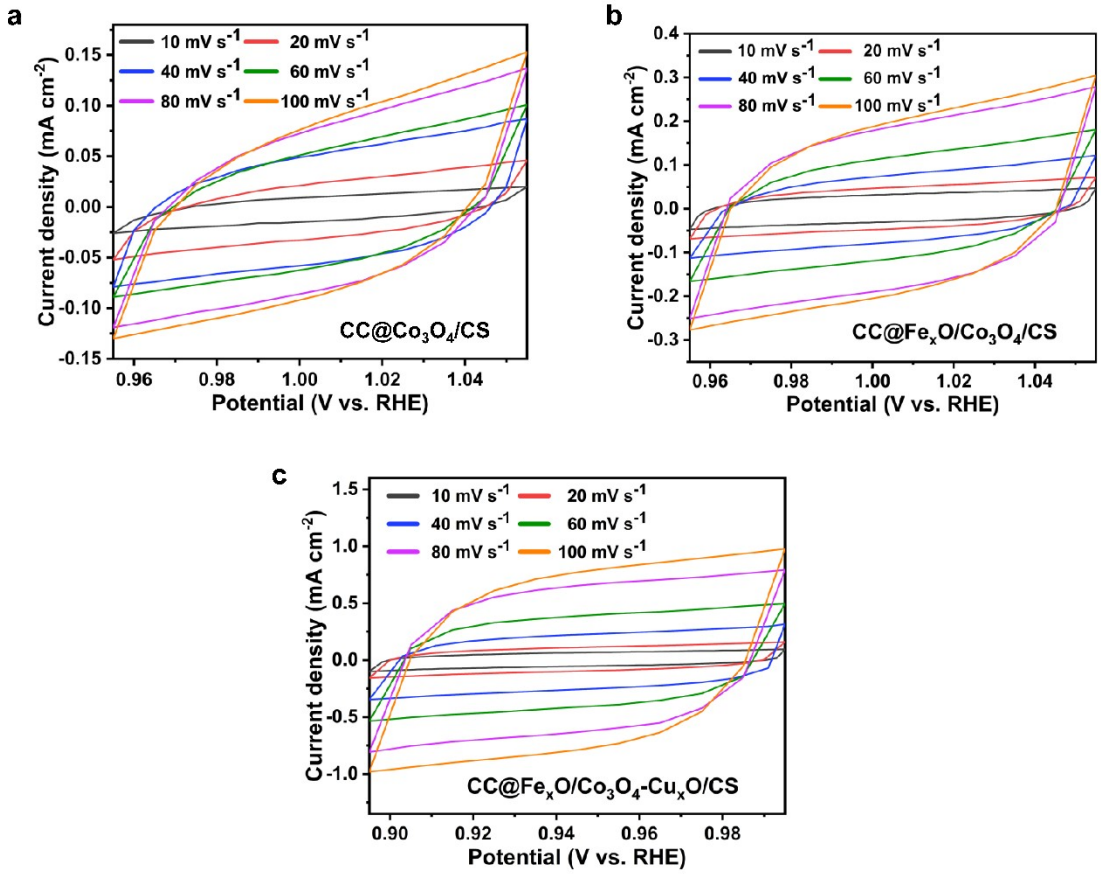

Fig. S5. CV curves of CC@Co_3O_4/CS (a), CC@Fe_xO/Co_3O_4/CS (b) and CC@Fe_xO/Co_3O_4-Cu_xO/CS (c), respectively.

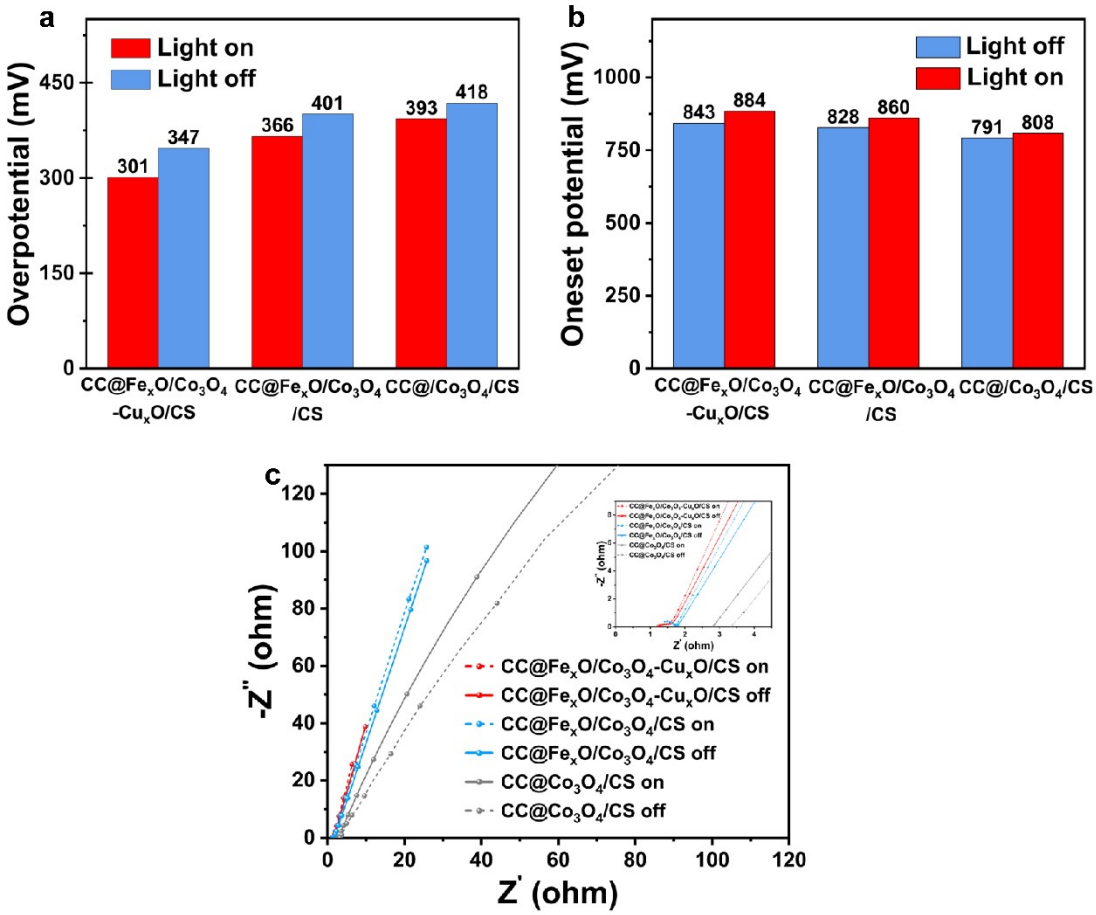

Fig. S6. The overpotentials and onset potentials for OER (a) and ORR (b) of the CC@Fe_xO/Co_3O_4-Cu_xO/CS samples before and after light illumination, along with the EIS spectra (c) of CC@Co_3O_4/CS, CC@Fe_xO/Co_3O_4/CS, and CC@Fe_xO/Co_3O_4-Cu_xO/CS under both dark and illuminated conditions.

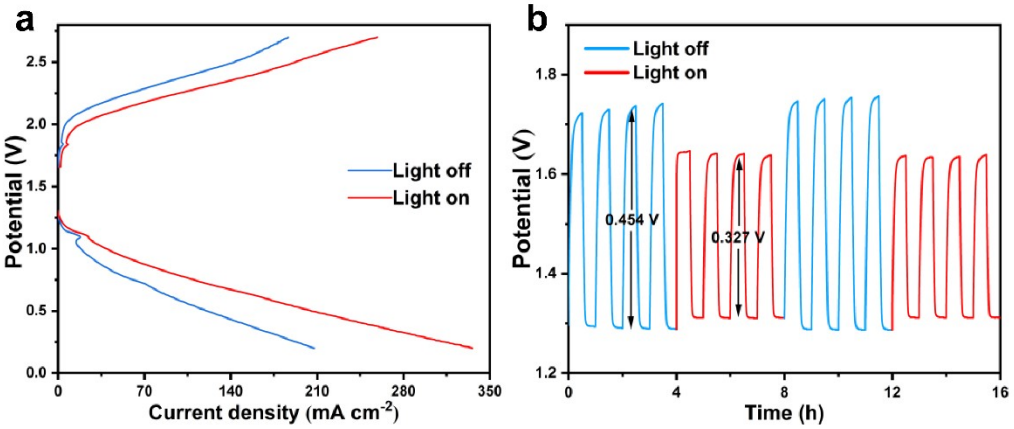

Fig. S7. The charge-discharge polarization curves (a), and short-term cycle tests (b) of CC@Fe_xO/Co_3O_4-Cu_xO/CS ZABs.

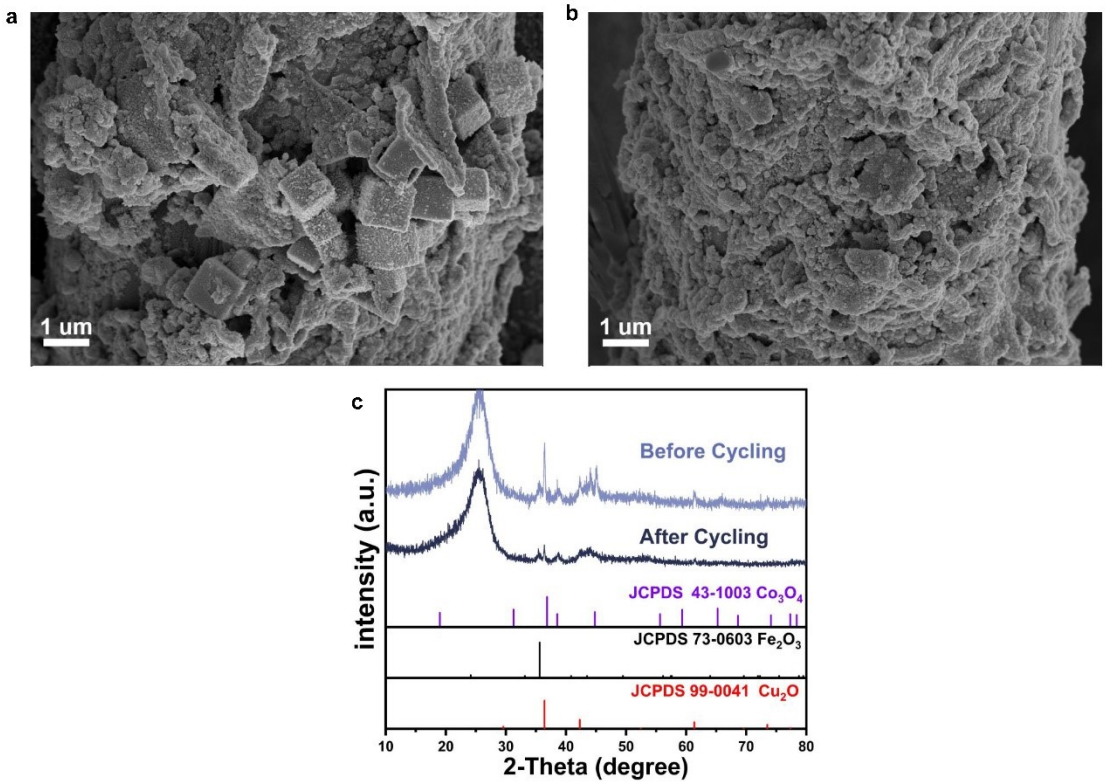

Fig. S8. The microstructural morphology after 48 h (a) and 96 h (b) cyclic testing, and XRD patterns (c) of the CC@Fe_xO/Co_3O_4-Cu_xO/CS cathode after stability testing.

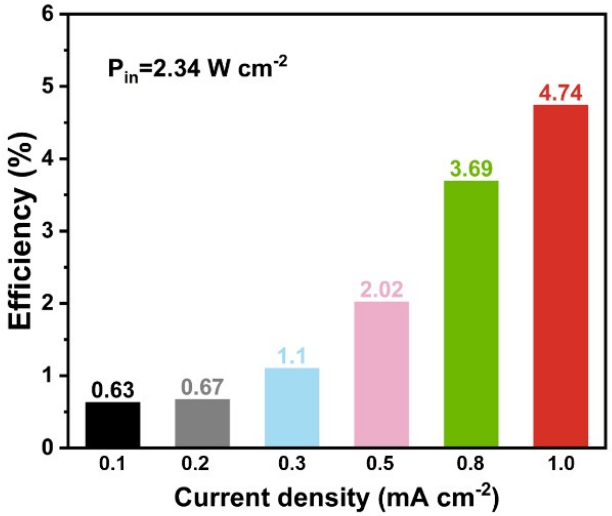

Fig. S9. Power conversion efficiencies of Zn-air battery with CC@Fe_xO/Co_3O_4-Cu_xO/CS as photocathodes at different current densities under 2.34 W·cm^{-2} illumination.

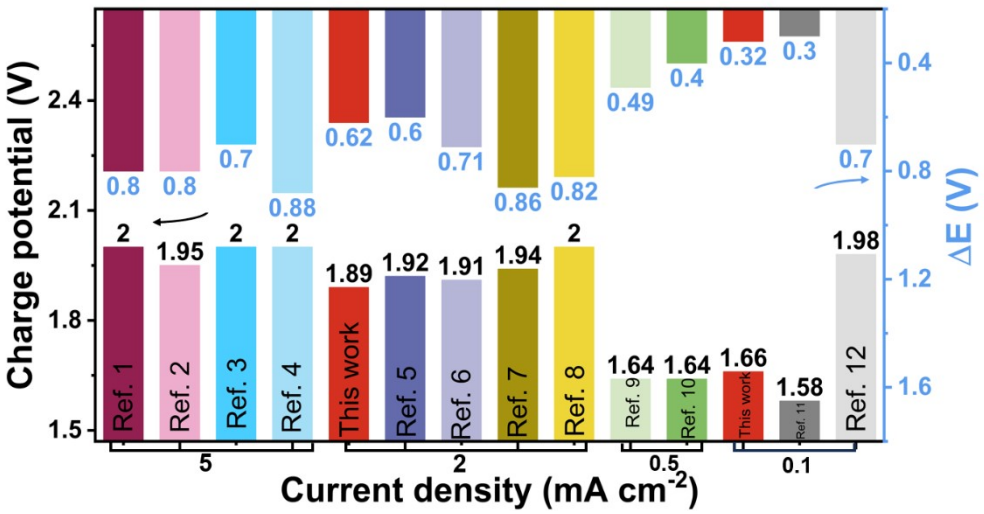

Fig. S10. Comparison chart of CC@Fe_xO/Co_3O_4-Cu_xO/CS ZABs with previously reported ZABs.

Notes and references

1 C. Tomon, S. Sarawutanukul, S. Duangdangchote, *Chem Commun,* 2019, **55,** 5855-5858.

2 S. Sarawutanukul, C. Tomon, S. Duangdangchote, *Batteries & Supercaps,* 2020, **3,** 541-547.

3 R. Ren, G. Liu, J. Y. Kim, R. E. A. Ardhi, M. X. Tran, W. Yang, J. K. Lee, *Appl. Catal.,* B 2022, **306,** 121096.

4 R. Ren, G. Liu, J. Y. Kim, *Applied Catalysis B: Environmental,* 2022, **306,** 121096.

5 X. Liu, Y. Yuan, J. Liu, B. Liu, X. Chen, J. Ding, X. Han, Y. Deng, C. Zhong, W. Hu, *Nat. Commun.* 2019, **10,** 4767.

6 S. Liang, L. J. Zheng, L. N. Song, X. X. Wang, W. B. Tu, J. J. Xu, *Adv. Mater.* 2023, **36,** 2307790.

7 Y. Wu, Y. Ding, M. Chen, H. Zhang, J. Yu, T. Jiang, M. Wu, *Small* 2024, **20,** 2408627.

8 T. Zhu, C. Xia, B. Wu, J. Pan, H. Yang, W. Zhang, B. Y. Xia, *Appl. Catal. B Environ. Energy* 2024, **357,** 124315.

9 L. Luo, R. Tang, L. Su, J. Kou, X. Guo, Y. Li, X. Cao, J. Cui, S. Gong, *Energy Storage Mater.* **2024**, 72, 103773.

10 X. Cao, Y. Gao, Z. Wang, H. Zeng, Y. Song, S. Tang, L. Luo, S. Gong, *ACS Appl. Mater. Interfaces* **2023**, 15, 32365.

11 M.-D. Hao, Q. Li, J.-H. Sun, D. Liu, H.-L. Yu, R. Liu, *Rare Met.* **2025**, 44, 2836.

12 D. H. Wu, M. Ul Haq, L. Zhang, J. J. Feng, F. Yang, A. J. Wang, *J. Colloid Interface Sci.* **2024**, 662, 149.